деформаций при последовательном изменении размеров моделируемой полости. Зоны разрушения определяются по критерию прочности Хоека-Брауна. Численное моделирование выполнено для различных горно-геологических условий и размеров выработки. Для построения обобщающих зависимостей используется метод нелинейного оценивания, сочетающий множественную регрессию и дисперсионный анализ.

Результаты. Выполнены многовариантные расчеты напряженно-деформированного состояния области, содержащей струговую лаву и демонтажную камеру, для различных значений прочности пород, мощности угольного пласта, глубины разработки и размеров демонтажного штрека. Полученные результаты обобщены для различных горно-геологических условий в виде зависимостей высоты зон разрушения и перемещений контура демонтажной камеры от перечисленных выше факторов.

Научная новизна. Впервые установлены закономерности развития деформаций и формирования зон разрушения в породном массиве в окрестности демонтажной камеры в момент сопряжения с забоем струговой лавы. Получены расчетные формулы для определения основных геомеханических характеристик, необходимых для выбора способа крепления демонтажной камеры в различных горно-геологических условиях.

Практическая значимость. Совокупность формул для определения основных геомеханических характеристик составляет инженерную методику определения нагрузки на крепь демонтажной камеры, а также является основой типовых материалов проектирования демонтажных камер струговых лав в условиях Западного Донбасса.

Ключевые слова: *демонтажная камера, струговая лава, напряженно-деформированное состояние, критерий прочности*.

Рекомендовано до публікації докт. техн. наук С.М.Гапєєвим. Дата надходження рукопису 20.03.15.

Xiongming Lai[1],
Jianhang Su[1],
Cheng Wang[1,2],
Yong Zhang[1],
He Huang[1]

1 – Huaqiao University, Xiamen, China
2 – Xi'an Jiaotong University, Xi'an, China

GENERAL MOST PROBABLE POINT BASED APPROACH FOR RELIABILITY INDEX COMPUTATION

Сюнмін Лай[1],
Цзяньхан Су[1],
Чен Ван[1, 2],
Юн Чжан[1],
Хе Хуан[1]

1 – Університет Хуацяо, м. Сяминь, КНР
3 – Сіаньський транспортний (Цзяотун) університет, м. Сіань, КНР

УНІВЕРСАЛЬНИЙ ПІДХІД ДО РОЗРАХУНКУ КОЕФІЦІЄНТА НАДІЙНОСТІ, ЩО ГРУНТУЄТЬСЯ НА НАЙІМОВІРНІШИХ ЗНАЧЕННЯХ

Purpose. As for the reliability analysis of complex engineer problems, the nonlinearity and implicitness of the limit state functions always stand in the way. On one hand, the nonlinearity influences the convergence computation of some reliability problems when using most methods of reliability analysis. On the other hand, the implicitness means that information of the partial derivatives of the limit state function is impossible to obtain, which is necessary for most of the reliability methods. In order to overcome these difficulties, the paper presents a new general most probable point based (MPP-based) approach for computing the reliability.

Methodology. Within the framework of the proposed iterative algorithm, we presented new strategies for searching three types of the approximate MPPs by merely using the input and output information of the limit state function. In addition, the found MPPs can be used for updating the constructed response surface of the limit state function, which in its turn helps to find a more accurate MPP.

Findings. As illustrated by the examples, the proposed method provides excellent precision and convergence for the calculation results.

Originality. Three types of the approximate MPPs are firstly presented for updating the constructed response surface of the limit state function, whose input and output information is sufficient.

Practical value. The proposed method does not necessitate any requirements for the detailed format and complexity of the limit state functions, which is an advantage. Hence, it is especially applicable to the implicit case of complex engineer problems.

Keywords: *limit state function, most probable point, index computation*

© Xiongming Lai, Jianhang Su, Cheng Wang, Yong Zhang, He Huang, 2016

Introduction. As for design engineers, the reliability analysis necessitates the design procedure due to uncertainties of control and prediction on influential factors in engineering design. During the last twenty years, the theory and methods of mechanical reliability have been developed significantly. Generally, the two types of methods are available for reliability analysis [1]. The first type contains the 'analytical' methods that are based on the concept of an MPP of failure. A case in point is the Rackwitz-Fiessler [2] algorithm (or called the JC method), which is suggested by Joint Committee on Structural Safety (JCSS) as the standard method for engineering application. However, such methods are not applicable to the case of the implicit limit state functions, which should be solved by numerical simulation. Furthermore, the convergence of computation cannot be guaranteed for tackling some practical nonlinear reliability problems. With regard to these difficulties, Monte Carlo sampling methods, as the second type, are widely used. Although a very powerful method, Direct Monte Carlo Simulation (DMCS), is computationally too demanding for assessing the probability of failure. Because of the inefficiency of DMCS, several variance-reduction methods such as importance sampling [3], subset simulation [4], line sampling [5] and so on have been developed in the past in order to improve the computation precision and efficiency [6]. The Monte Carlo simulation and the improved methods mentioned above are universally valid to most reliability problems. However, as compared to the 'analytical' methods, their computation are still to some degree large-scale.

Instead of using Monte Carlo sampling methods, this paper presents another general MPP-based approach, which does not necessitate any requirements for the detailed format and complexity of the limit state functions. In fact, the proposed method can find more accurate MPP based on initial properly chosen failure points on the failure surface according to certain strategies. Hence, it is especially applicable to the implicit case. Besides, compared with the prevailing standard JC method, the new method excels in computation convergence as proved by the examples in this paper.

Reliability theory. The reliability computation includes the evaluation of integrals over arbitrary non-dimensional continuous joint Probability Density Function (PDF), shown as follows

$$p_f = \int_{G(x)=\leq 0} f_x(x_1, x_2, ..., x_n) dx_1 \cdot dx_2 ... dx_n, \qquad (1)$$

where p_f is the probability of failure; $\mathbf{x} = (x_1, x_2, \ldots, x_n)$ denotes n arbitrary independent random variables; $f_x(x_1, x_2, \ldots, x_n)$ represents the joint PDF of $x_1, x_2, \ldots, x_n$; $G(\mathbf{x})$ is the limit state function (or performance function). It is defined so that it is negative for the states whose probability is being calculated.

Generally, the mechanical models (such as mechanical structure, mechanism and so on) are too complex, and there exits the inaccessible explicit analytical expression for the performance function. Meanwhile, $f_x(x_1, x_2, \ldots, x_n)$ $dx_1 \cdot dx_2 \ldots dx_n$ in (1) usually involves high multi-dimensional integration. Hence, direct computation of (1) is difficult. From the perspective of convenience, equation (2) is easier for reliability computation than(1).

$$\min \beta = \left(\sum_{i=1}^{n} u_i^2 \right)^{1/2}$$
$$\text{subject to } g(\mathbf{u}) = 0, \qquad (2)$$

where the uncorrelated normalized variable $\mathbf{u} = \mathbf{T}(x)$. $\mathbf{T}$ is a generally nonlinear transformation that depends on the types of random distribution of X. For more details, please see Rosenblatt's transformation [7], respectively. The reliability index β can be defined as the distance from the origin to the MPP $\mathbf{u}^*$, which is the closest point on the boundary of the performance function $g(\mathbf{u}) = 0$ in the standard normal space, as shown by Fig. 1.

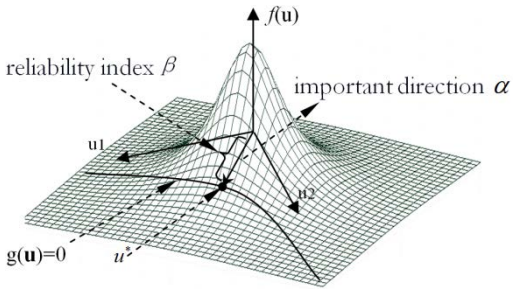

Fig. 1. The reliability index β represented by the minimum distance from the origin to the boundary of the performance function $g(\mathbf{u}) = 0$

Once the MPP $\mathbf{u}^*$ and the reliability index β are found, probability of failure p_f can be computed as follows.

$$p_f = \Phi(-\beta). \qquad (3)$$

The FORM method is developed based on (2) and its iterative algorithm can be expressed as

$$\beta^k = \frac{g(\mathbf{u}^k) - (\nabla_{\mathbf{u}} g(\mathbf{u}^k))^T \mathbf{u}^k}{\| \nabla_{\mathbf{u}} g(\mathbf{u}^k) \|}; \qquad (4)$$

$$\boldsymbol{\alpha}^k = \frac{\nabla_{\mathbf{u}} g(\mathbf{u}^k)}{\| \nabla_{\mathbf{u}} g(\mathbf{u}^k) \|}; \qquad (5)$$

$$\mathbf{u}^{k+1} = -\beta^k \boldsymbol{\alpha}^k, \qquad (6)$$

where $\mathbf{u}^k$ is the *k-th* iterative point of the MPP $\mathbf{u}^*$; β^k is the *k-th* iterative index of the reliability index β; $\boldsymbol{\alpha}^k$ is the *k-th* iterative vector of the important vector $\boldsymbol{\alpha}$ and its direction is set as the minus gradient of the limit state function $g(\mathbf{u})$ at $\mathbf{u}^k$. The direction of $\mathbf{u}^{k+1}$ is the same as $\boldsymbol{\alpha}^k$. The above iterative process of (4–6) is expressed in Fig. 2.

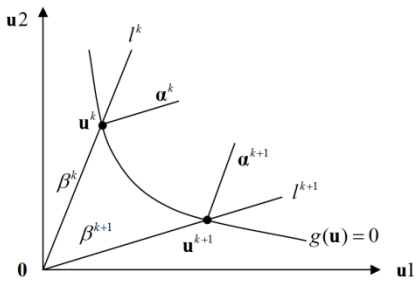

Fig. 2. The iterative process of the reliability index β and the MPP $\mathbf{u}^*$ in the standard normal space

In Fig. 2, the direction of the line l^{k+1} is chosen as that of $\boldsymbol{\alpha}^k$. And $\mathbf{u}^{k+1}$ is the intersection between the line l^{k+1} and the limit state function $g(\mathbf{u}) = 0$. If the nonlinearity of the limit state function $g(\mathbf{u}) = 0$ is strong, the above iterative process may diverge. For example, the limit state function $g(\mathbf{u}) = 0$ in Fig. 3 is quite nonlinear. And the direction of the line l^{k+2} is the same as $\boldsymbol{\alpha}^{k+1}$. Apparently, there exists no intersections between the line l^{k+2} and the limit state function $g(\mathbf{u}) = 0$. Hence, the FORM method fails in this situation. The fact of the matter is that its ability of searching the MPP $\mathbf{u}^*$ is not competent for the nonlinear reliability problem. In the following paper, a new method is proposed for finding the MPP $\mathbf{u}^*$ based on three strategies. The numerical examples in the following paper verify that the three strategies together have a more preferable ability to search the MPP $\mathbf{u}^*$.

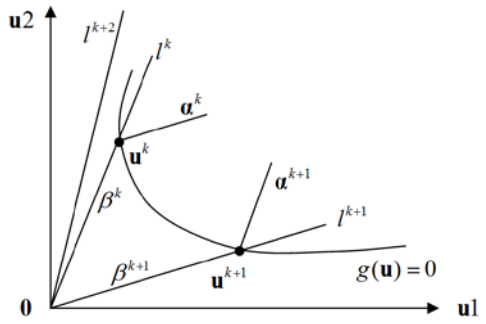

Fig. 3.The divergent iterative process of the reliability index β*and the MPP* $\mathbf{u}^*$ *in the standard normal space*

The proposed methodology. For the sake of convenience, arbitrary random variables $\mathbf{x}$ in reliability problems can be transformed to the standard normal $\mathbf{u}$ by means of the nonlinear transformation $\mathbf{T}$. Let us find the MPP $\mathbf{u}^*$ in standard normal space. Firstly, at the step $k = 0th$, find the initial points $\left\{\mathbf{u}_j^{(0)}(j = 1...m)\right\}$ on the boundary of the limit state function. Secondly, at the step $k > 0th$, find the MPP $\mathbf{u}^*$ derived from the information provided by initial points $\left\{\mathbf{u}_j^{(0)}(j = 1...m)\right\}$ according to certain strategies.

Initial points obtained on the boundary of the limit state function. For the initial step $k = 0th$, choosing initial random points $\left\{\hat{\mathbf{u}}_j^{(0)}(j = 1...m)\right\}$ in standard normal space based on certain strategies could properly accelerate the convergence for computing the MPP to some degree. Especially, if the random points fall into the neighborhood of the MPP, it would be easier to find the MPP with the information provided by these random points. The direction $\boldsymbol{\alpha}$ from the origin of coordinate to the MPP in the failure domain is the important direction as shown in Fig. 1. The vector $\boldsymbol{\alpha}$ points to the direction, which has greatest impact on the limit state function in the standard normal space, and its expression is as follows

$$\boldsymbol{\alpha} = \frac{\partial g}{\partial \mathbf{u}^*} = \left[\frac{\partial g}{\partial u_1}, \frac{\partial g}{\partial u_2}, \ldots, \frac{\partial g}{\partial u_n}\right]^T \Big|_{\mathbf{u}^*}. \tag{7}$$

Shan, S. and Wang, G.G. [8] replaced the important direction $\frac{\partial g}{\partial \mathbf{u}^*}$ by $\frac{\partial g}{\partial \bar{\mathbf{u}}}$, where $\bar{\mathbf{u}}$ is the mean value. In this way, the inner loop for searching the MPP is avoided. Hence, the trivial nested optimization for reliability becomes the more efficient single loop optimization. Inspired by this, the paper finds the MPP towards this important direction. First, the finite difference method in (8) is used to approximate the gradient $\frac{\partial g}{\partial \mathbf{u}^*}$.

$$\frac{\partial g}{\partial u_i} = -\Big[g(\bar{u}_1, \ldots, \bar{u}_{i-1}, \bar{u}_i, \bar{u}_{i+1}, \ldots, \bar{u}_n) - g(\bar{u}_1, \ldots, \bar{u}_{i-1}, \bar{u}_i + \Delta u_i, \bar{u}_{i+1}, \ldots \bar{u}_n)\Big] \Big/ \Delta u_i \; (i = 1 \sim n). \tag{8}$$

If the limit state function should be solved by the numerical simulation, then $n + 1$ times simulations are required.

After that, the paper builds a line l_0 through the origin with the above rough approximation as the direction.

$$l_0 : \frac{u_1}{\frac{\partial g}{\partial u_1}} = \frac{u_2}{\frac{\partial g}{\partial u_2}} = \ldots = \frac{u_n}{\frac{\partial g}{\partial u_n}} = t_0. \tag{9}$$

At this time, there is an intersection $\mathbf{u}_\times$ between the line l_0 and the limit state function $g(\mathbf{u}) = 0$, as depicted in Fig. 4.

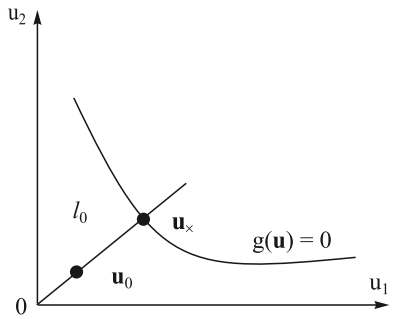

Fig. 4. The intersection point $\mathbf{u}_\times$ *between the line* l_0 *and the limit state function* $g(\mathbf{u}) = 0$

In engineering applications, the limit state function $g(\mathbf{u}) = 0$ is usually implicit and nonlinear. Direct solution of $\mathbf{u}_\times$ through $g(\mathbf{u}) = 0$ and lines l_0 are not easy. However, numerical iterative solutions are possible by means of the secant method as shown in (10).

$$\begin{gathered} t^{p+2} = t^{p+1} - \frac{(t^{p+1} - t^p)}{(g^{p+1} - g^p)} g^{p+1}; \\ \mathbf{u}^{p+2} = t^{p+2} * \mathbf{u}_0; \\ g^{p+2} = g(\mathbf{u}^{p+2}); \\ g^0 = g(\mathbf{0}), \quad g^1 = g(\mathbf{u}_0); \\ t^0 = 0, \quad t^1 = 1. \end{gathered} \tag{10}$$

Where u_0 is a point chosen on the line l_0 $\mathbf{0}$ is a zero vector with $1 \times n$.

Once the intersection $\mathbf{u}_\times$ is found, generate n random point $\left\{\hat{\mathbf{u}}_j^{(0)}(j = 1...m)\right\}$ around $u_\times$ according to (11) as the initial starts at the step $k = 0th$.

$$\hat{\mathbf{u}}_j^{(0)} = \mathbf{u}_\times + C * \gamma_{rand} * \boldsymbol{\sigma}, \tag{11}$$

where $\boldsymbol{\sigma} = [\sigma_{x1}, \sigma_{x2}, \ldots, \sigma_{xn}]$ is the standard deviation of random variables $\mathbf{x}$; γ_{rand} is a random value ranging from –1 to 1; C is a coefficient being the value equal to 0.1 in this paper.

The lines $\{l_j(j = 1, \ldots, m)\}$ between origin and $\left\{\hat{\mathbf{u}}_j^{(0)}(j = 1...m)\right\}$ can be obtained, shown as follows.

$$l_j : \frac{u_{j,1}}{\hat{u}_{j,1}^{(0)}} = \frac{u_{j,2}}{\hat{u}_{j,2}^{(0)}} = \ldots = \frac{u_{j,n}}{\hat{u}_{j,n}^{(0)}} = t_j (j = 1, \ldots, m). \tag{12}$$

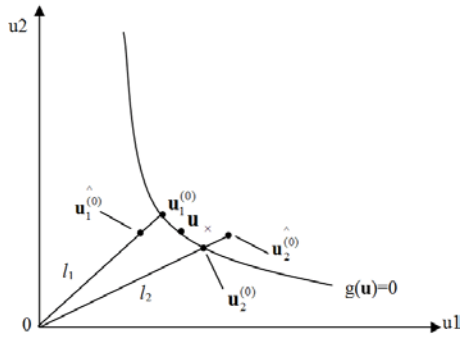

Fig. 5. The points $\mathbf{u}_1^{(0)}$, $\mathbf{u}_2^{(0)}$ *on the boundary* $g(\mathbf{u}) = 0$ *derived from random points* $\mathbf{u}_1^{(0)}$, $\mathbf{u}_2^{(0)}$ *at the step* $k = 0$*th in two-dimensional case*

Likewise, the intersections $\left\{\mathbf{u}_j^{(0)}(j = 1, ..., m)\right\}$ around the point $\mathbf{u}_\times$ can be also derived from lines $\{l_j(j = 1, \ldots, m)\}$ and the limit state function $g(\mathbf{u}) = 0$. The above process is shown in Fig. 5 with the two-dimensional case. By using the secant method shown in (13), the initial intersections points $\left\{\mathbf{u}_j^{(0)}(j = 1, ..., m)\right\}$ can be computed.

$$\begin{gathered} t_j^{p+2} = t_j^{p+1} - \frac{(t_j^{p+1} - t_j^p)}{(g_j^{p+1} - g_j^p)} g_j^{p+1}; \\ \mathbf{u}_j^{p+2} = t_j^{p+2} * \hat{\mathbf{u}}_j^{(0)}; \\ g_j^{p+2} = g(\mathbf{u}_j^{p+2}); \\ g_j^0 = g(\mathbf{0}), \quad g_j^1 = g(\hat{\mathbf{u}}_j^{(0)}); \\ t_j^0 = 0, \quad t_j^1 = 1. \end{gathered} \tag{13}$$

Sometimes, $\frac{\partial g}{\partial \mathbf{u}^*}$ appears very unequal to $\frac{\partial g}{\partial \mathbf{u}}$, since there is no intersection between $\{l_j(j = 1, \ldots, m)\}$ and the limit state function $g(\mathbf{u}) = 0$. As shown in Fig. 6, the contour line of $g(\mathbf{u})$ is the example 2 with the parameter $P = 1$ in the further described example 2. The $\mathbf{n1}_\perp = \frac{\partial g}{\partial \mathbf{u}_0}$ and $\mathbf{n2}_\perp = \frac{\partial g}{\partial \mathbf{u}^*}$ are the gradients of $g(\mathbf{u})$ at the origin and the MPP, respectively. Obviously, both are very unequal. There are no intersections $\mathbf{u}_\times$ between the limit state function $g(\mathbf{u}) = 0$ and the line l_0 along the direction of $\mathbf{n1}_\perp$. In other words, no solutions can be found in (10) for this case. Hence, the above method cannot find the initial points $\left\{\mathbf{u}_j^{(0)}(j = 1, ..., m)\right\}$ on the boundary of the limit state function $g(\mathbf{u}) = 0$.

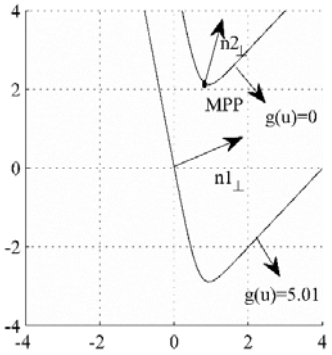

Fig. 6. No intersection points $\mathbf{u}_\times$ *between the limit state function* $g(\mathbf{u}) = 0$ *and the line* l_0 *along the direction of* $\mathbf{n1}_\perp$

This case directly generates random points $\left\{\hat{\mathbf{u}}_j^{(0)}(j = 1...m)\right\}$ computed by (14) and work out the intersections $\mathbf{u}_j^{(0)}$ by the secant method. Repeat the above 2 steps, until n points $\left\{\mathbf{u}_j^{(0)}(j = 1, ..., m)\right\}$ on the limit state function $g(\mathbf{u}) = 0$ are found.

$$\hat{\mathbf{u}}_j^{(0)} = C * \gamma_{rand} * \boldsymbol{\sigma}(j = 1 \ldots m). \tag{14}$$

Finally, the distance between the origin and $\left\{\mathbf{u}_j^{(0)}(j = 1, ..., m)\right\}$ are acquired by (15).

$$\beta_j^{(0)} = \left\|\mathbf{u}_j^{(0)}\right\| (j = 1, ..., m). \tag{15}$$

New strategies for searching the new MPP. The new strategies for generating the new MPP is based on the limited information of the above initial points $\left\{\mathbf{u}_j^{(0)}(j = 1, ..., m)\right\}$ on the limit state function $g(\mathbf{u}) = 0$. The paper presents three methods for searching different types of the new points as the newest MPP under different situations at the *k-th* step.

The I-type point. At the *k-th* step, the available information contains $\left\{\mathbf{u}_j^{(k)}(j = 1, ..., m)\right\}$, $\left\{\beta_j^{(k)}(j = 1, ..., m)\right\}$. The middle point $\bar{\mathbf{u}}^{(k)}$ as the average position of $\left\{\mathbf{u}_j^{(k)}(j = 1, ..., m)\right\}$ is figured out by (16).

$$\bar{\mathbf{u}}^{(k)} = \frac{1}{m} \sum_{j=1}^{m} \mathbf{u}_j^{(k)}. \tag{16}$$

Then follow the aforementioned secant method in Section 3.1, the new line $l_{1-new}^{(k)}$, the new intersection $\mathbf{u}_{1-new}^{(k)}$ and the new reliability index $\beta_{1-new}^{(k)}$ can be obtained, as illustrated by Fig. 7.

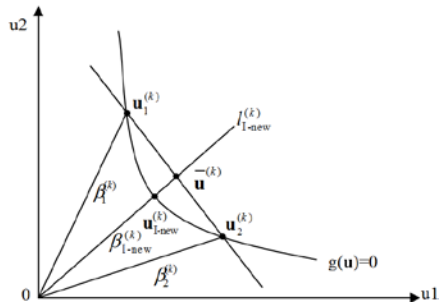

Fig. 7. The new MPP $\mathbf{u}_{\text{I}-new}^{(k)}$ *is derived from points* $\mathbf{u}_1^{(k)}$, $\mathbf{u}_2^{(k)}$ *on the boundary* $g(\mathbf{u}) = 0$ *at the kth step in two-dimensional case*

Supposing $\beta_q^{(k)} = \max\left\{\beta_j^{(k)}(j = 1, ..., m)\right\}$, if the new reliability index $\beta_{\text{I}-new}^{(k)}$ corresponding to the new intersection $\mathbf{u}_{\text{I}-new}^{(k)}$ is smaller than $\beta_q^{(k)}$, then substitute $\mathbf{u}_q^{(k)}$ and $\beta_q^{(k)}$ for $\mathbf{u}_{\text{I}-new}^{(k)}$ and $\beta_{\text{I}-new}^{(k)}$ respectively in $\left\{\mathbf{u}_j^{(k)}(j = 1, ..., m)\right\}$ and $\left\{\beta_j^{(k)}(j = 1, ..., m)\right\}$.

The method concentrates on finding the local optimum point within the local space (or called the internal space) covered by the existing points $\left\{\mathbf{u}_j^{(k)}(j = 1, ..., m)\right\}$.

The II-type point.

From Fig. 8, we can find that there exists no I-type point $\mathbf{u}_{\text{I}-new}^{(k)}$, since the local optimum point cannot be found within the internal space covered by $\mathbf{u}_1^{(k)}$ and $\mathbf{u}_2^{(k)}$. Hence, for that case, the first method is infeasible.

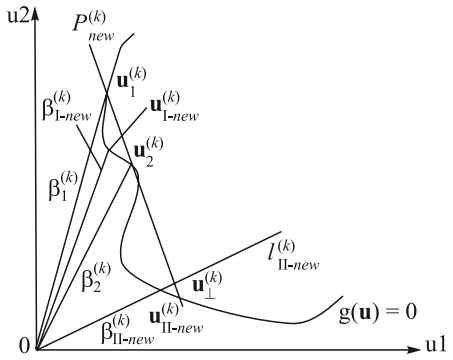

Fig. 8. The second method for searching the new MPP $\mathbf{u}_{\text{II}-new}^{(k)}$ *based on points* $\mathbf{u}_1^{(k)}$, $\mathbf{u}_2^{(k)}$ *on the boundary* $g(\mathbf{u}) = 0$ *at the k-th step in two-dimensional case*

The second method is suggested for searching a new MPP. In Fig. 8, it constructs a new hyperplane through points $\left\{\mathbf{u}_j^{(k)}(j = 1, ..., m)\right\}$ at the *k-th* step. The equation of the hyperplane $P^{(k)}$ is

$$P^{(k)} = \begin{vmatrix} u_1 & \cdots & u_n & 1 \\ u_{11}^{(k)} & \cdots & u_{1n}^{(k)} & 1 \\ \cdots & \cdots & \cdots & \cdots \\ u_{m1}^{(k)} & & u_{mn}^{(k)} & 1 \end{vmatrix} = 0. \qquad (17)$$

The expansion of (17) can be expressed as

$$D_1^{(k)}u_1 + D_2^{(k)}u_2 + \ldots D_n^{(k)}u_n + D_{n+1}^{(k)} = 0, \qquad (18)$$

where $D_q^{(k)}(q = 1, 2, \ldots, n)$ is the cofactor of the element $u_q (q = 1, 2, \ldots, n)$, respectively in determinant $P^{(k)}$ and is defined as $D_q^{(k)} = (-1)^{j+1} M_{1j}^{(k)}$. Here $M_{1j}^{(k)}$ is the minor of the element u_q of determinant $P^{(k)}$.

The new line $l_{\text{II}-new}^{(k)}$ through the origin and perpendicular to the hyperplane $P^{(k)}$ is

$$l_{\text{II}-new}^{(k)} : \frac{u_1}{D_1^{(k)}} = \frac{u_2}{D_2^{(k)}} = \ldots = \frac{u_n}{D_n^{(k)}}. \qquad (19)$$

Also, using the secant method in (10), the new MPP $\mathbf{u}_{\text{II}-new}^{(k)}$ (called the II-type point) is available.

Supposing $\beta_q^{(k)} = \max\left\{\beta_j^{(k)}(j = 1, \ldots, m)\right\}$, if the new reliability index $\beta_{\text{II}-new}^{(k)}$ derived from $\mathbf{u}_{\text{II}-new}^{(k)}$ is smaller than $\beta_q^{(k)}$, then renew $\left\{\mathbf{u}_j^{(k)}(j = 1, ..., m)\right\}$ and $\left\{\beta_j^{(k)}(j = 1, \ldots, m)\right\}$ by substituting $\mathbf{u}_q^{(k)}$ and $\beta_q^{(k)}$ for $\mathbf{u}_{\text{II}-new}^{(k)}$ and $\beta_{\text{II}-new}^{(k)}$, respectively.

The III-type point.

In Fig. 9, the new MPP $\mathbf{u}_{\text{II}-new}^{(k)}$ searched by the second method is obviously not the optimum point. Instead, the optimum point lies in area A. Hence, the paper presents the third method to find it.

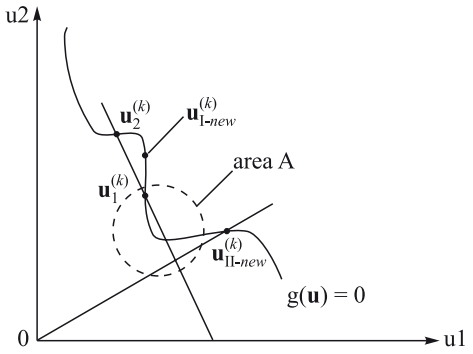

Fig. 9. The new MPP $\mathbf{u}_{\text{II}-new}^{(k)}$ *searched by the second method is the optimum point in two-dimensional case*

As can be seen from Fig. 10, two vectors are built based on the best point $\mathbf{u}_{best}^{(k)}$, which are closest to the origin in $\left\{\mathbf{u}_j^{(k)}(j = 1, ..., m)\right\}$. In Fig. 10, $\mathbf{u}_1^{(k)}$ closer to the origin is better than $\mathbf{u}_2^{(k)}$ in two-dimensional case and $\mathbf{u}_{best}^{(k)} = \mathbf{u}_1^{(k)}$. One vector is $n_\beta^{(k)}$ being from the MPP to the origin of coordinate. The other is the normal vector $\mathbf{n}_\perp^{(k)}$ of the hyper plane $P^{(k)}$ constructed by $\left\{\mathbf{u}_j^{(k)}(j = 1, ..., m)\right\}$. The resultant vector $\mathbf{n}_\eta^{(k)}$ and its opposite vector $\mathbf{n}_{-\eta}^{(k)}$ can be acquired by the above two vectors.

Fig. 11 is partial enlargement of area *A* in Fig. 10. Along the direction of $\mathbf{n}_\eta^{(k)}$, the $\mathbf{u}_{new}^{(k,h)}$ is computed by (20).

$$\mathbf{u}_{new}^{(k,h)} = \mathbf{u}_{best}^{(k)} + \frac{C_0}{2^h}\mathbf{n}_\eta^{(k)}(h = 0, 1, ...). \qquad (20)$$

Where $\mathbf{u}_{new}^{(k,h)}$ is the iterative point at the *h-th*step; C_0 is the initial step length and can be chosen according to the actual problems.

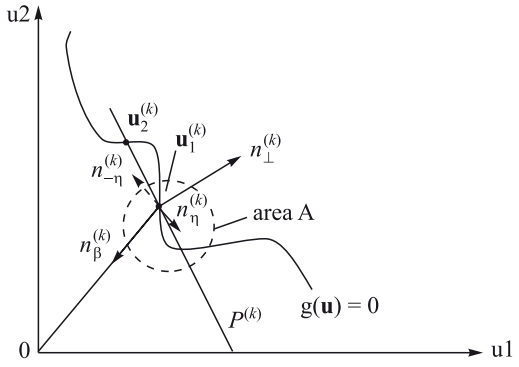

Fig. 10. The third method to find the new MPP in two-dimensional case

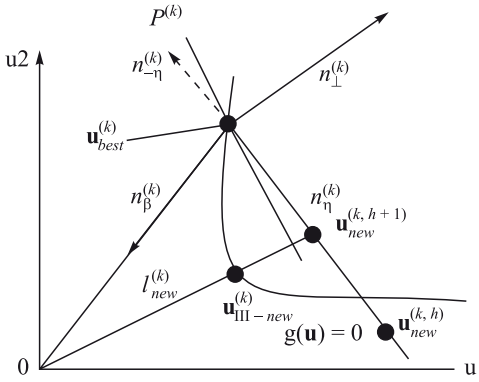

Fig. 11. The third method to find the new MPP in two-dimensional case

Likewise, the $\mathbf{u}_{-new}^{(k,h)}$ along the direction of $\mathbf{n}_{-\eta}^{(k)}$ can be also obtained by (21).

$$\mathbf{u}_{-new}^{(k,h)} = \mathbf{u}_{best}^{(k)} - \frac{C_0}{2^h}\mathbf{n}_{-\eta}^{(k)}(h = 0,1,...). \qquad (21)$$

Repeatedly compute (20) and (21) by increasing the integer h until $g(\mathbf{u}_{new}^{(k,h)}) < 0$ or $g(\mathbf{u}_{-new}^{(k,h)}) < 0$, which means that a new point within the failure domain is found. After that, builds the new line $l_{new}^{(k)}$ through the origin and $\mathbf{u}_{new}^{(k,h)}$ (or $\mathbf{u}_{-new}^{(k,h)}$). By means of the secant method presented above, the III-type point $\mathbf{u}_{\text{III}-new}^{(k)}$ intersects between the limit state function $g(\mathbf{u}) = 0$ and the line $l_{new}^{(k)}$ can be found.

Supposing $\beta_q^{(k)} = \max\left\{\beta_j^{(k)}(j = 1,...,m)\right\}$, if the new reliability index $\beta_{\text{III}-new}^{(k)}$ derived from $\mathbf{u}_{\text{III}-new}^{(k)}$ is smaller than $\beta_q^{(k)}$, then renew $\left\{\mathbf{u}_j^{(k)}(j = 1,...,m)\right\}$ and $\left\{\beta_j^{(k)}(j = 1,...,m)\right\}$ by substituting $\mathbf{u}_q^{(k)}$ and $\beta_q^{(k)}$ for $\mathbf{u}_{\text{III}-new}^{(k)}$ and $\beta_{\text{III}-new}^{(k)}$, respectively.

As for the second method, its jumping ability is relatively larger than that of the third method. In other words, the II-type point $\mathbf{u}_{\text{II}-new}^{(k)}$ is usually far from the internal space covered by $\left\{\mathbf{u}_j^{(k)}(j = 1,...,m)\right\}$, as can be seen in Fig. 8. Hence, the external space neighboring the internal space will be missed by the second method, while the third method fills this vacancy. By combining both methods, the ability of the external optimization in the external space complementary to the internal space accelerates. Therefore, the first method is responsible for the internal optimization and the others for the external optimization. These entire methods together carry out the global optimization for searching the MPP.

The procedure for the proposed algorithm. The following process makes up the proposed algorithm for reliability analysis, utilizing the above-described strategies for searching the new MPP.

1. Generate initial points $\left\{\hat{\mathbf{u}}_j^{(0)}(j = 1...m)\right\}$ properly in standard normal space at the *kth step* = 0*th*.

2. By means of the method for searching different types of the new points that was presented above, find the new MPP based on the information $\left\{\mathbf{u}_j^{(k)}(j = 1,...,m)\right\}$ and $\left\{\beta_j^{(k)}(j = 1,\ldots,m)\right\}$ derived from the *kth* step.

3. If $\left|\beta_{\max}^{(k)} - \beta_{\min}^{(k)}\right| / \beta_{\min}^{(k)} < \varepsilon$, the algorithm would have converged. Here, $\beta_{\min}^{(k)} = \min\left\{\beta_j^{(k)}(j = 1,...,m)\right\}$, $\beta_{\max}^{(k)} = \max\left\{\beta_j^{(k)}(j = 1,...,m)\right\}$.

For more details, please refer to Fig. 12.

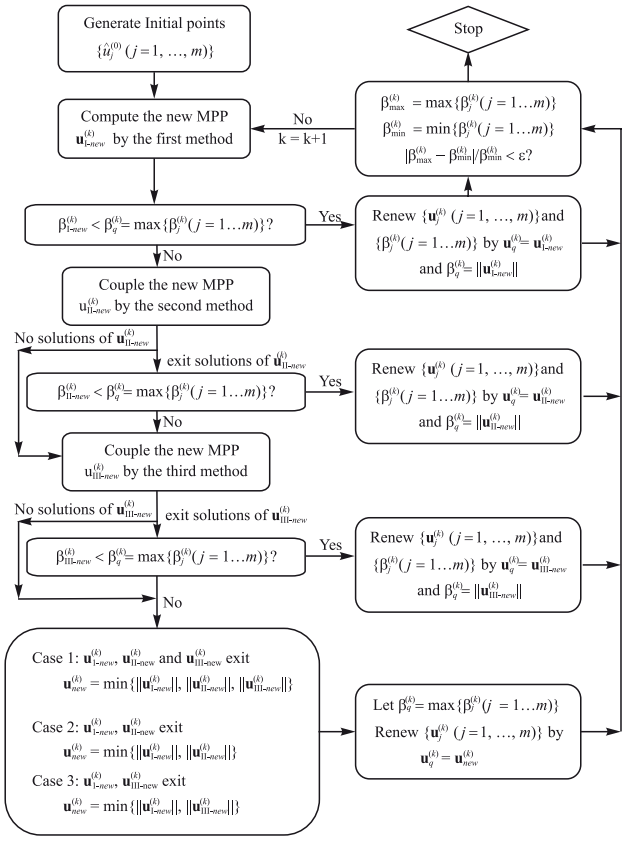

Fig. 12. The procedure for the proposed algorithm

Numerical example. A number of examples are used to demonstrate the superiority of the presented method. To show the accuracy and the computational effectiveness, example 1 is used for comparing the results computed by the JC method and the Monte Carlo method. While example 2 and 3 show that the presented method has excellent convergence for high nonlinear limit state functions, which can't be solved by the JC method. Lastly, example 4 demonstrates that the presented method is quite suitable for the complex implicit reliability problems in engineering applications.

Example 1. A cantilever beam made of isotropic material, as shown in Fig. 13, is subjected to a distributed transverse load [9].

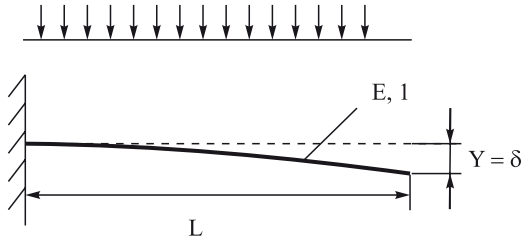

Fig. 13. A cantilever beam

The performance function of the tip displacement is expressed as

$$\delta = G(X) = QL^4/(8EI) - 4,$$

where $X = [Q, L, E, I]^T$, in which Q is the constant distributed transverse load acting on the beam, L symbolizes the length of the beam, E is the Young's modulus of the beam material, and I is the moment of the cross-section. Q, L, E, I are normally distributed and their distribution parameters are provided in Table 1.

Different methods are used to compute the example. The sampling size for the Monte Carlo method is 10^7. The results are shown in Table 2. The reliability results computed by the proposed method are quite close to those of the others.

Example 2. Consider a highly nonlinear limit state function [10]

$$G(x) = (1/P)\ln\{\exp[P(1 + x_1 - x_2)] + \\ + \exp[P(5 - 5x_1 - x_2)]\},$$

where $x_1 \sim N(0, 1)$ and $x_2 \sim N(0, 1)$. P is a parameter with $P = 1$ or $P = 10$. As the limit state function is nonlinear as shown in Fig. 14, the JC method cannot solve it due to nonconvergence. A new method based on the explicit gradient function of the limit state function was presented to compute the example [10]. In this paper, only the output response of limit state function rather than its explicit gradient function is used. The results of the both methods are the same. The reliability indices are 2.2995 and 1.8455, respectively corresponding to $P = 1$ and $P = 10$.

Table 1

The distribution parameters of the basic random variables in example 1

	Mean (μ)	Standard Deviation (σ)	Distribution
Q N/m	1*e*4	3*e*3	Normal
L m	5	2*e*–3	Normal
E (N/m^2)	7.3*e*10	1*e*9	Normal
I (m^4)	1.067*e*–3	1*e*–7	Normal

Table 2

The reliability results of example 1

Method	*Pf*	Relative error
JC	0.02255	0.4 %
The proposed P_{Lf}	0.02255	0.4 %
Monte Carlo	0.02251–	

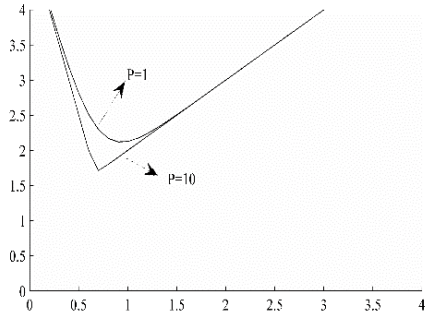

Fig. 14. The limit state function of example 2

Example 3. Consider another highly nonlinear limit state function

$$G(x) = g(x) = x_1^3 + x_2^3 - 4,$$

where $x_1 \sim N(3, 1)$ and $x_1 \sim N(2.9, 1)$. The JC method cannot solve it as well. However, the presented method well solves it with the result of the reliability index 2.3909. Because the difference between the mean of and is very small. For the sake of approximate estimation, supposing $\overline{x_1} = \overline{x_2} = 2.95$, the MPP is $u_1^* = u_2^* = 1.69$, where y_1 and y_2 are the standard normal variables transformed from x_1 and x_2. Fig. 15 shows the limit state function in the standard normal space. The approximate reliability index is $\beta = \sqrt{2}\left|u_1^*\right| = 2.3902$, which is almost the same as that computed by the presented method.

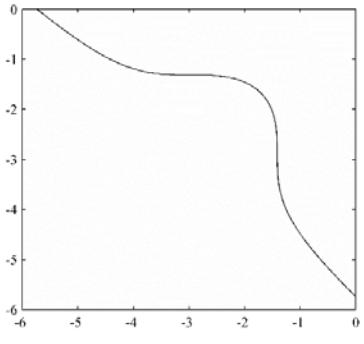

Fig. 15. The limit state function of example 3

Example 4. As for the turning machine, the drive-enabling reliability (DER) and the kinematic precision reliability (KDPR) of the angle displacement errors Δ_θ are investigated. The original data are taken from the paper written by Lai, X.M. and Duan, J. [3]. As shown in Fig. 16, the turning machine is assembled on the machine frame at the assemblage Point1 and Point2.

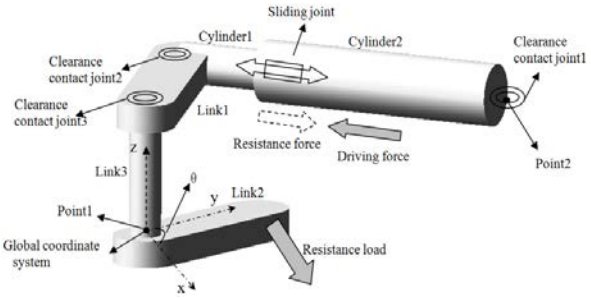

Fig. 16. The turning machine

The driver (composed of Cylinder1 and Cylinder2) generates driving force to overcome the resistance force (RF) derived from resistance loads. The driving speed is about 0.015 m/s and last 8s. During the running process, the mean values and standard deviations of the main influential factors are given in Table 3.

In the research of Lai, X. M. and Duan, J. [3], the theory for computing the DER and KDPR was studied. As for the mechanism, its limit state functions for DER and KDPR are implicit, and they were solved by numerical simulation [3]. Then it resorted to the Monte Carlo based method, which is the important sampling method to compute the DER and KDPR. In this paper, the output responses of the limit state functions are also solved by numerical simulation. However, the DER and KDPR of the mechanism are solved by the presented method. As shown in Table 4, the reliability results of the proposed method are quite close to those in the mentioned research [3]. Hence, this example shows the excellent accuracy and the computational effectiveness of the proposed method for implicit cases, which often are met in engineering applications.

Table 3

Influential factors of the turning machine

	Nominal value (or mean) of input parameters	Range of input parameters (Δ)	Standard Deviation
Dimensional size	L1 = 0.255 m L2 = 0.354 m	±0.001 m	Δ/3
Coordinate	Point1_x = 0.65 m Point1_y = 0.5 m Point2_x = 0.99 m Point2_y = 1 m	±0.001 m	
Friction coefficient (μ)	u1 ~ u4 = 0.1	±0.01	
Clearance size	C1 ~ C3 = 0.0005 m	±0.0001 m	
Resistance loads(RF)	RF = 5000 N	±50 N	
Velocity of driver	V = 0.015 m/s	±0.001/s	
Driving force	DF = 4260N	10 N	
Angle displacement tolerance	1°	±0.2°	

Table 4

The reliability results of DER and KDPR

Probability of failure (10^{-4})	DER	KDPR
Method in Ref. 3	6.25	2.148
The proposed method	6.26	2.146

Conclusion. A general MPP-based method is presented for computing the reliability problems. The concept and the implementation of the presented method are explained in details. The method is constructed based on searching the new MPP by merely resorting to the output response of the limit state function. No explicit gradient functions of the limit state function are used in the whole searching process. Hence, the new method is applicable to complex implicit engineering problems, which should be solved by numerical simulation e. g. finite element analysis. As shown by the examples, the presented approach has excellent convergence for nonlinear problems, which are met in engineering design quite often. Since the new method has no requirements (e. g. nonlinear or linear, explicit or implicit) for the limit state functions, it is a general method, which is suitable for most engineering applications.

Acknowledgements. This work was financially supported by National Natural Science Foundation of China (Grant No. 51305143, Grant No. 51205141, Grant No. 51205141, Grant No. 51305142, Grant No. 51405168), the Start-up Foundation of High-talent Research Project from Huaqiao University (Grant No. 12BS204), Natural Science Foundation of Fujian Province of China (No. 2014J01191), the General Financial Grant from the China Postdoctoral Science Foundation (Grant No: 2014M552429), project of Xiamen science and technology plan (3502Z20143041), introduction of talents Huaqiao University Scientific Research Projects (Project No. 12BS217) and the Promotion Program for Young and Middle-aged Teachers in Science and Technology Research at Huaqiao University under Grant ZQN-PY212.

References / Список літератури

1. Bichon, B. J., McFarland, J. M. and Mahadevan, S., 2011. Efficient surrogate models for reliability analysis of systems with multiple failure modes, *Reliability Engineering and System Safety*, vol. 96, pp. 1386–1395.

2. Gu, X. G. and Lu, J. W., 2014. Reliability-based robust assessment for multiobjective optimization design of improving occupant restraint system performance. *Computers in Industry*, vol. 65, no. 8, pp. 1169−1180.

3. Lai, X. M. and Duan, J., 2011. Probabilistic approach to mechanism reliability with multi-influencing factors. In: *Proc. of the Institution of Mechanical Engineers, Part C, Journal of Mechanical Engineering Science*, vol. 225, no. C12, pp. 2991–2996.

4. Song, S. F., Lu, Z. Z. and Qiao, H. W., 2009. Subset simulation for structural reliability sensitivity analysis. *Reliability Engineering & System Safety*, vol. 94, no.2, pp. 658–665.

5. Lu, Z. Z., Song, S. F., Yue, Z. F. and Wang, J., 2008. Reliability sensitivity method by line sampling. *Structural Safety*, vol. 30, no. 6, pp. 517–532.

6. Rubinstein, R.Y. and Kroese, D.P., 2007. Simulation and the Monte Carlo Method. *Hoboken, New Jersey: John Wiley & Sons, Inc*.
7. Shahraki, A.F. and Noorossana, R., 2014. Reliability-based robust design optimization: A general methodology using genetic algorithm. *Computers & Industrial Engineering*, vol. 74, no. 1, pp. 199–207.
8. Shan, S. and Wang, G.G. 2008. Reliable design space and complete single-loop reliability-based design optimization. *Reliability Engineering & System Safety*, vol. 93, no. 8, pp. 1218–1230.
9. Huang, B.Q. and Du, X.P., 2008. Probabilistic uncertainty analysis by mean-value first order Saddle point Approximation. *Reliability Engineering & System Safety*, vol. 93, no. 2, pp. 325–336.
10. Di, W. and Ding, G. 2005. A search algorithm for structural reliability index. *Chinese Journal of Computational Mechanics*, vol. 22, no. 6, pp. 788–791.

Мета. При аналізі надійності у складних інженерних завданнях, нелінійність і неявність функцій граничного стану завжди створюють перешкоди. З одного боку, нелінійність впливає на обчислення збіжності деяких завдань забезпечення надійності при використанні більшості методів аналізу надійності. З іншого боку, неявність означає, що інформацію щодо приватних похідних функції граничного стану неможливо отримати, проте вона необхідна для більшості методів забезпечення надійності. Для подолання цих труднощів, у роботі запропонований новий загальний підхід до обчислення надійності на основі найбільш вірогідного значення (MPP).

Методика. У рамках пропонованого ітераційного алгоритму ми представляємо нові стратегії для пошуку трьох типів приблизних найвірогідніших значень, використовуючи вхідну й вихідну інформацію про функції граничного стану. Знайдені найвірогідніші значення можуть бути використані для коригування побудованої поверхні відгуку функції граничного стану, що, у свою чергу, допомагає знайти найбільш точне найвірогідніше значення.

Результати. Як показано на прикладах, пропонований спосіб забезпечує чудову точність і збіжність результатів обчислень.

Наукова новизна. Уперше представлені три види приблизних найвірогідніших значень для коригування побудованої поверхні відгуку функції граничного стану за достатньої кількості вхідної та вихідної інформації.

Практична значимість. Перевага пропонованого способу у відсутності яких-небудь вимог до детального формату та складності функції граничного стану. Отже, він особливо добре застосовний у разі неявних складних інженерних завдань.

Ключові слова: *функція граничного стану, найвірогідніше значення, розрахунок індексів*

Цель. При анализе надежности в сложных инженерных задачах, нелинейность и неявность функций предельного состояния всегда создают препятствия. С одной стороны, нелинейность влияет на вычисление сходимости некоторых задач обеспечения надёжности при использовании большинства методов анализа надежности. С другой стороны, неявность означает, что информацию о частных производных функции предельного состояния невозможно получить, однако она необходима для большинства методов обеспечения надежности. Для преодоления этих трудностей, в работе предложен новый общий подход к вычислению надежности на основе наиболее вероятного значения (MPP).

Методика. В рамках предлагаемого итерационного алгоритма мы представляем новые стратегии для поиска трех типов приблизительных наиболее вероятных значений, используя входную и выходную информацию о функции предельного состояния. Найденные наиболее вероятные значения могут быть использованы для корректировки построенной поверхности отклика функции предельного состояния, что, в свою очередь, помогает найти более точное наиболее вероятное значение.

Результаты. Как показано на примерах, предлагаемый способ обеспечивает превосходную точность и сходимость результатов вычислений.

Научная новизна. Впервые представлены три вида приблизительных наиболее вероятных значений для корректировки построенной поверхности отклика функции предельного состояния при достаточном количестве входной и выходной информации.

Практическая значимость. Преимущество предлагаемого способа в отсутствии каких-либо требований к подробному формату и сложности функции предельного состояния. Следовательно, он особенно хорошо применим в случае неявных сложных инженерных задач.

Ключевые слова: *функция предельного состояния, наиболее вероятное значение, расчёт индексов.*

Рекомендовано до публікації докт. техн. наук В.В.Гнатушенком Дата надходження рукопису 15.04.15.